Supplementary Materials

Self-templated construction of 1D NiMo nanowires via a Li electrochemical tuning method for hydrogen evolution reaction

Dekang Huang,[ab†] Shu Li,[a†] Yanzhu Luo,[a] Li Liao,[a] Jinhua Ye,*[b] and Hao Chen*[a]

[a]College of Science, Huazhong Agricultural University, Wuhan 430070, PR China

[b]International Center for Materials Nanoarchitectonics (WPI-MANA), National Institute for Materials Science (NIMS), 1-1 Namiki, Tsukuba, Ibaraki 305-0044, Japan

E-mail: Jinhua.YE@nims.go.jp (J. Ye), hchenhao@mail.hzau.edu.cn (H. Chen)

[†]These authors contributed equally to this work.

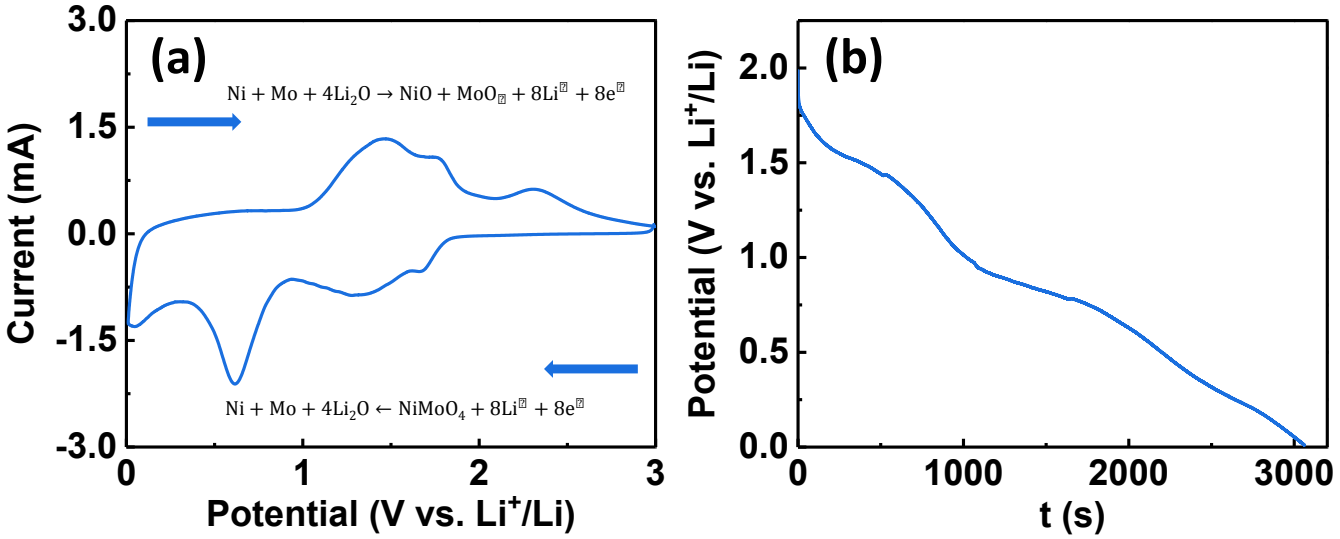

Fig. S1 (a) Cyclic voltammogram of the $NiMoO_4$/Ni foam electrode for the initial cycle at a scan rate of 0.1 mV s^{-1} in the potential window of 0.01-3.0 V; (b) discharge curve of the $NiMoO_4$/Ni foam electrode.

As shown in Fig. S1a, in the cathodic sweep, there are three reduction peaks at 1.68 V, 1.33 V, and 0.62 V, which can be assigned to Li insertion into the lattice of $NiMoO_4$ crystal structure, the formation of metallic Ni and Mo nanoparticles, and the generation of a solid-electrolyte interphase (SEI) layer, respectively. In the anodic sweep, another three peaks are observed, which can be attributed to the oxidation of metallic Ni and Mo to NiO and MoO_3, respectively. Fig. S1b displays the discharge curve of the $NiMoO_4$/Ni foam electrode at the current density of 0.1 mA cm^{-2}, in which the plateaus coincide well with the reduction peaks in Fig. S1a.

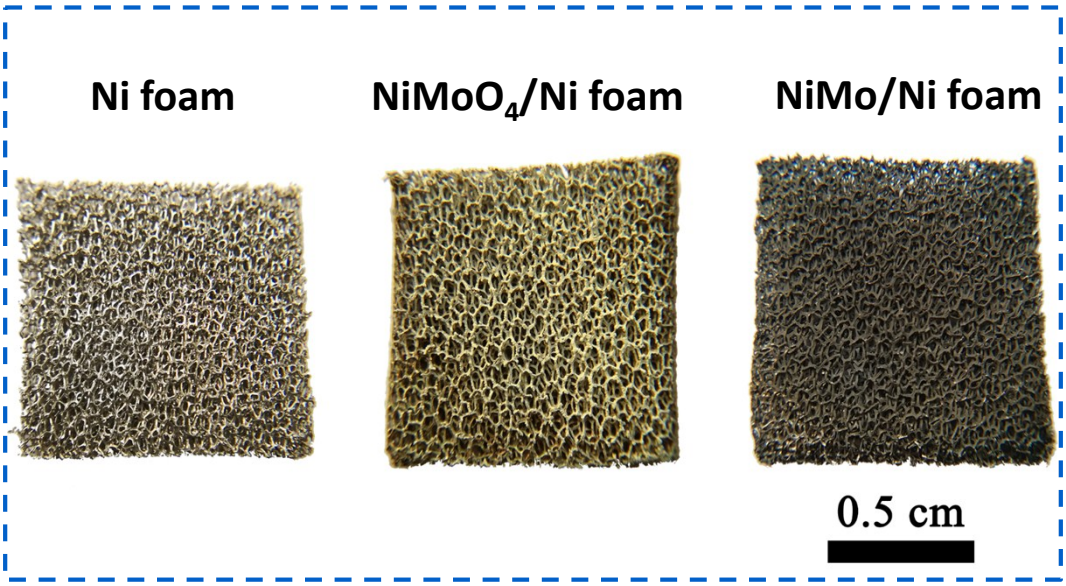

Fig. S2 Digital images of Ni foam, $NiMoO_4$/Ni foam, and NiMo/Ni foam.

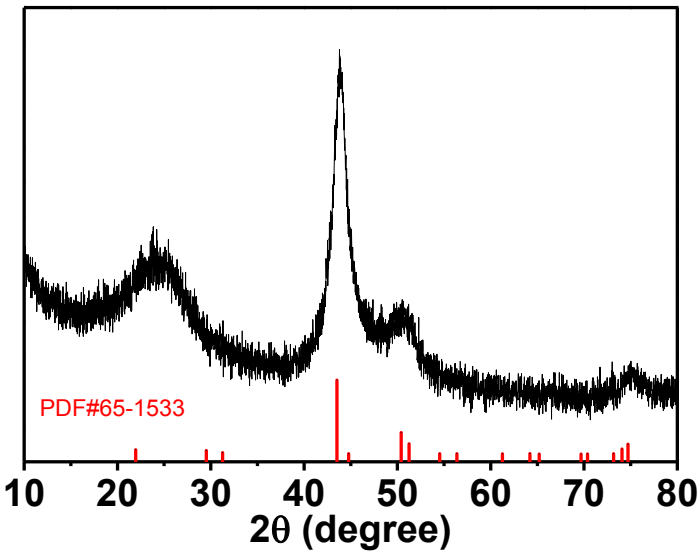

Fig. S3 XRD pattern of C-NiMo supported on the commercial carbon cloth (CC).

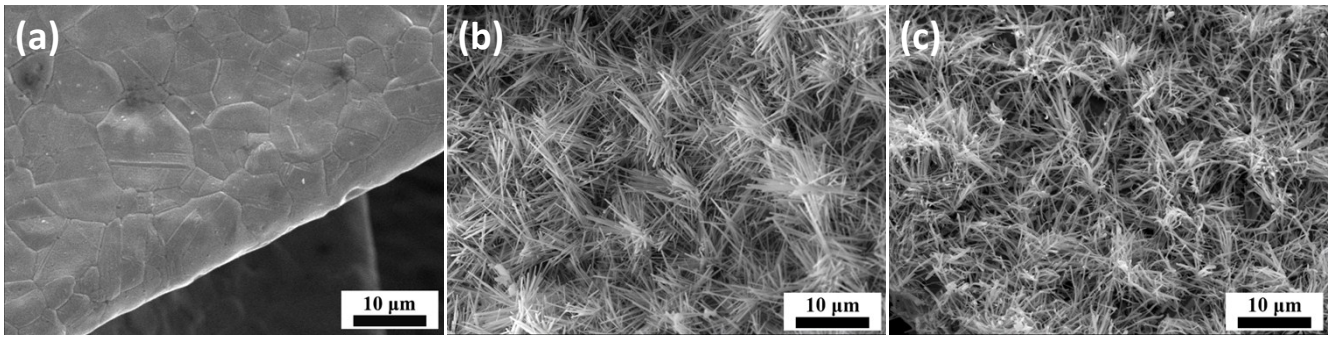

Fig. S4 Low-magnification FESEM images of Ni foam (a), $NiMoO_4$/Ni foam (b), and NiMo/Ni foam (c).

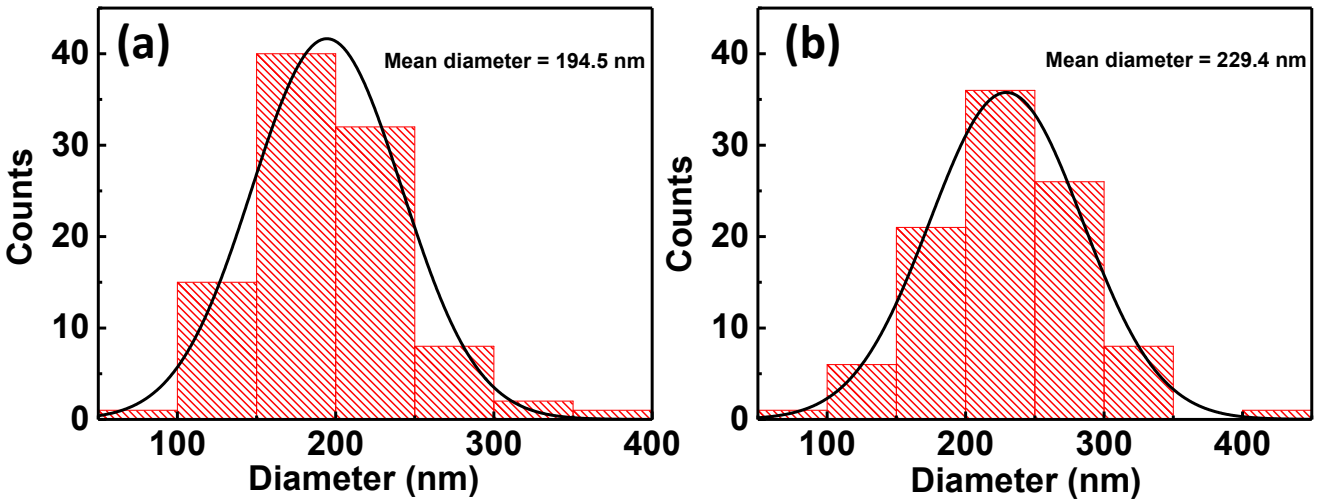

Fig. S5 Diameter distribution histograms for $NiMoO_4$ (a) and NiMo (b).

100 nanorods and nanowires in Fig. 1c and 1d were randomly selected and manually measured to obtain the diameter distribution histograms.

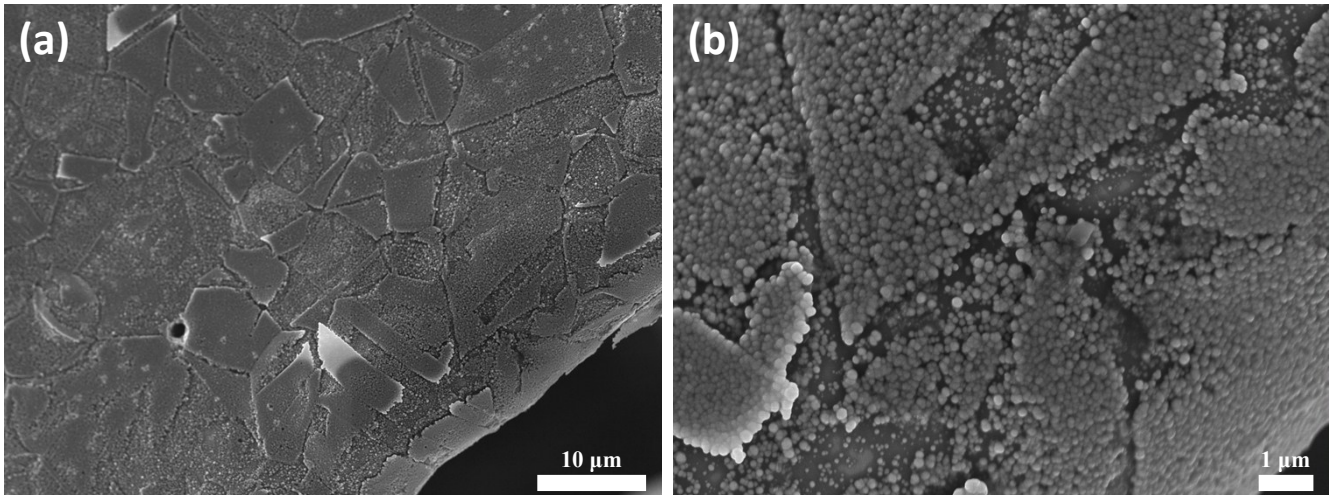

Fig. S6 (a, b) FESEM images of C-NiMo/Ni foam.

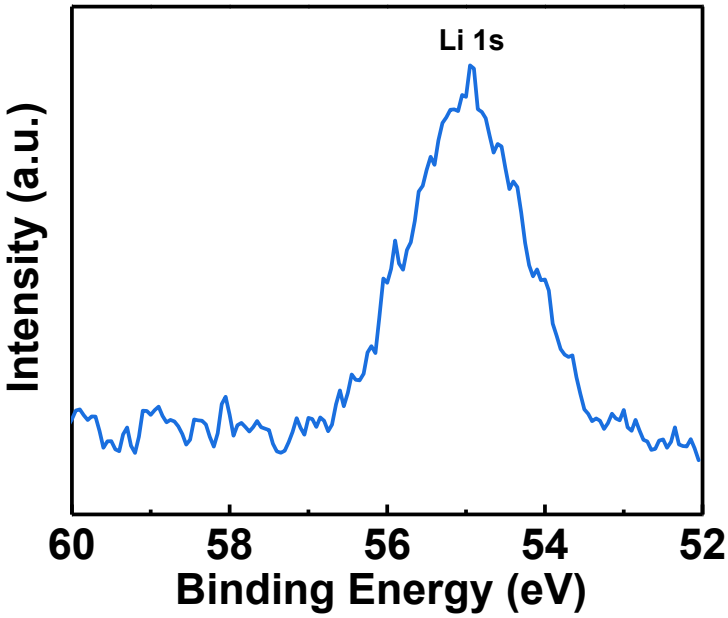

Fig. S7 High resolution of Li 1s spectrum of NiMo without Ar ion etching treatment.

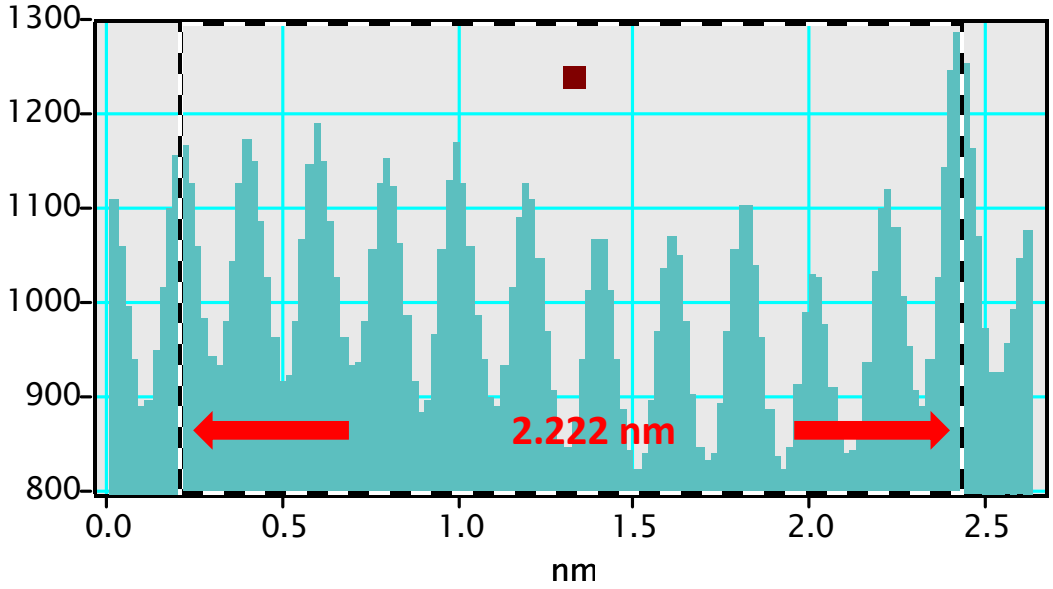

Fig. S8 Line-scanning profile of high magnification TEM image of $NiMoO_4$, indicating a lattice fringe spacing of 0.202 nm.

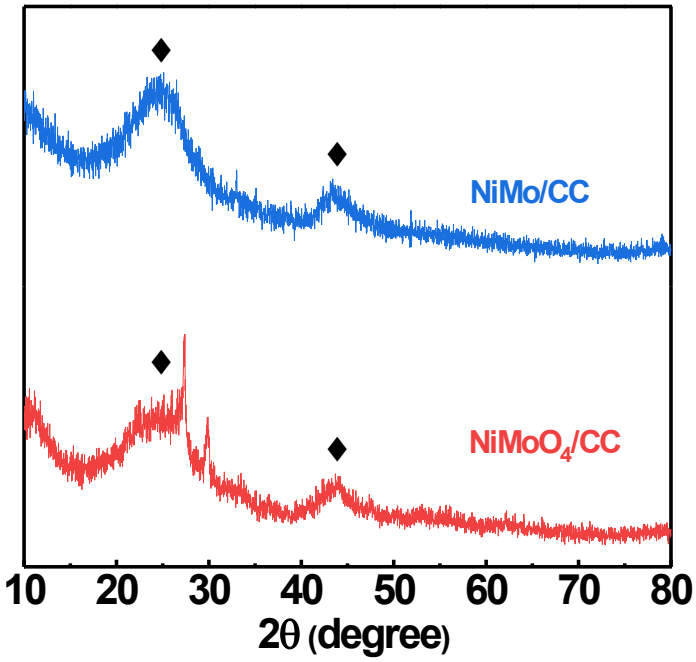

Fig. S9 XRD patterns of $NiMoO_4$ and NiMo supported on the commercial carbon cloth (CC).

The broad two peaks at 24.6° and 43.2° (marked with diamonds) were attributed to the (002) and (100) planes of graphitic carbon, respectively.

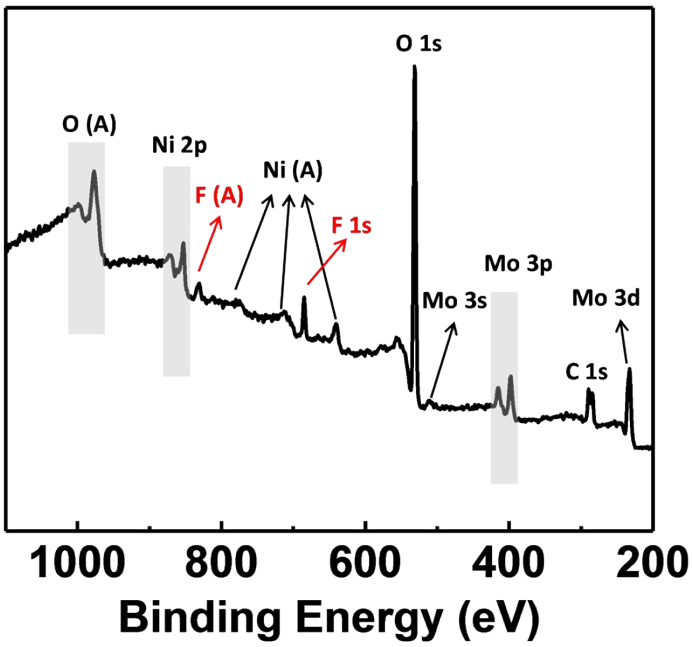

Fig. S10 XPS survey spectrum of NiMo/Ni foam without Ar ion etching treatment.

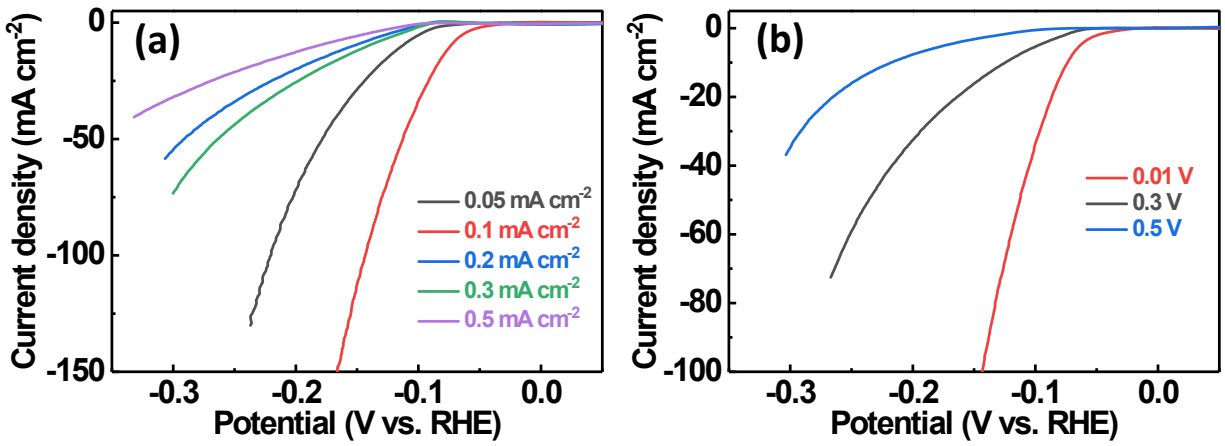

Fig. S11 LSV curves of NiMo samples prepared under different discharge current densities (a) and cut-off potentials (b).

Table S1. Comparison of HER activity for various NiMo HER electrocatalysts.

Catalyst	Loading (mg cm^{-2})	Tafel slope (mV dec^{-1})	η (mV) at j=10 mA cm^{-2}	Electrolyte	Reference
NiMo/Ni foam	**0.88**	**37.2**	**73**	**1 M KOH**	**This work**
MoNi microspheres	N/A	36.6	72	1 M KOH	1
$Mo_{0.6}Ni_{0.4}$	0.05	72	65	1 M KOH	2
Holey graphene covered NiMo	25.5	37	22	0.5 M H_2SO_4	3
NiMo-EDA	0.37	89	72	1 M KOH	4
Ni–Mo/Cu Nanowire	2.17	107	115	1 M KOH	5
Ni-Mo alloy nanosheet	0.8	45	35	1 M KOH	6
$MoNi_4/MoO_2$@Ni foam	~43.4	30	~15	1 M KOH	7
NC/NiMo/$NiMoO_x$/ Ni faom	~20	46	29	1 M KOH	8
Ni–Mo microspheres/Cu	4.2	49	47	1 M KOH	9
$MoNi_4/MoO_{3-x}$	8.7	36	17	1 M KOH	10
NiMo nanowires/Ni foam	0.41	86	30	1 M KOH	11
NiMo hollow nanorods	0.68	76	92	1 M KOH	12
Ni-Mo nanopowder	1	N/A	89	1 M NaOH	13
Ni_4Mo nanoclusters	1.2	78	76	1 M KOH	14
$MoNi_4$/Ni foam	1.09	36	~28	1 M KOH	15
NiMo/$NiMoO_4$/NC	~0.8	98.9	80	0.5 M H_2SO_4	16
NiMo-Mo_2C/C	0.75	73	[a]η_1=70	0.5 M H_2SO_4	17

[a] Overpotential at 1 mA cm^{-2}

Reference

1. Yang, L.; Zeng, L.; Liu, H.; Deng, Y.; Zhou, Z.; Yu, J.; Liu, H.; Zhou, W. Hierarchical microsphere of MoNi porous nanosheets as electrocatalyst and cocatalyst for hydrogen evolution reaction. Applied Catalysis B: Environmental, 2019, 249, 98-105.

2. Zhang, T.; Liu, X.; Cui, X.; Chen, M.; Liu, S.; Geng, B. Colloidal Synthesis of Mo-Ni Alloy Nanoparticles as Bifunctional Electrocatalysts for Efficient Overall Water Splitting. Advanced Materials Interfaces, 2018, 5(13), 1800359.

3. Ito, Y.; Ohto, T.; Hojo, D.; Wakisaka, M.; Nagata, Y.; Chen, L.; Hu, K.; Izumi, M.; Fujita, J.; Adschiri, T. Cooperation between holey graphene and NiMo alloy for hydrogen evolution in an acidic electrolyte. ACS Catalysis, 2018, 8(4), 3579-3586.

4. Gao, W.; Gou, W.; Zhou, X.; Ho, J. C.; Ma, Y.; Qu, Y. Amine-Modulated/Engineered Interfaces of NiMo Electrocatalysts for Improved Hydrogen Evolution Reaction in Alkaline Solutions. ACS Applied Materials & Interfaces, 2018, 10(2), 1728-1733.

5. Zhao, S.; Huang, J.; Liu, Y.; Shen, J.; Wang, H.; Yang, X.; Zhu, Y.; Li, C. Multimetallic Ni–Mo/Cu nanowires as nonprecious and efficient full water splitting catalyst. Journal of Materials Chemistry A, 2017, 5(8), 4207-4214.

6. Zhang, Q.; Li, P.; Zhou, D.; Chang, Z.; Kuang, Y.; Sun, X. Superaerophobic Ultrathin Ni-Mo Alloy Nanosheet Array from In Situ Topotactic Reduction for Hydrogen Evolution Reaction. Small, 2017, 13(41), 1701648.

7. Zhang, J.; Wang, T.; Liu, P.; Liao, Z.; Liu, S.; Zhuang, X.; Chen, M.; Zschech, E.; Feng, X. Efficient hydrogen production on $MoNi_4$ electrocatalysts with fast water dissociation kinetics. Nature Communications, 2017, 8, 15437.

8. Hou, J.; Wu, Y.; Cao, S.; Sun, Y.; Sun, L. Active Sites Intercalated Ultrathin Carbon Sheath on Nanowire Arrays as Integrated Core-Shell Architecture: Highly Efficient and Durable Electrocatalysts for Overall Water Splitting. Small, 2017, 13(46), 1702018.

9. Gao, M. Y.; Yang, C.; Zhang, Q. B.; Zeng, J. R.; Li, X. T.; Hua, Y. X.; Xu, C. Y.; Dong, P. Facile electrochemical preparation of self-supported porous Ni–Mo alloy microsphere films as efficient bifunctional electrocatalysts for water splitting. Journal of Materials Chemistry A, 2017, 5(12), 5797-5805.

10. Chen, Y.; Zhang, Y.; Zhang, X.; Tang, T.; Luo, H.; Niu, S.; Dai, Z.; Wan, L.; Hu, J. Self-Templated Fabrication of $MoNi_4/MoO_{3-x}$ Nanorod Arrays with Dual Active Components for Highly Efficient Hydrogen Evolution. Advanced Materials, 2017, 29(39), 1703311.

11. Fang, M.; Gao, W.; Dong, G.; Xia, Z.; Yip, S.; Qin, Y.; Qu, Y.; Ho, J. C. Hierarchical NiMo-based 3D electrocatalysts for highly-efficient hydrogen evolution in alkaline conditions. Nano Energy, 2016, 27, 247-254.

12. Tian, J.; Cheng, N.; Liu, Q.; Sun, X.; He, Y.; Asiri, A. M. Self-supported NiMo hollow nanorod array: an efficient 3D bifunctional catalytic electrode for overall water splitting. Journal of Materials Chemistry A, 2015, 3(40), 20056-20059.

13. Mckone, J. R.; Sadtler, B. F.; Werlang, C. A.; Lewis, N. S.; Gray, H. B. Ni–Mo Nanopowders for Efficient Electrochemical Hydrogen Evolution. ACS Catalysis, 2013, 3(2), 166-169.

14. Zhang, Y.; Ouyang, B.; Xu, K.; Xia, X.; Zhang, Z.; Rawat, R. S.; Fan, H. J. Prereduction of Metal Oxides via Carbon Plasma Treatment for Efficient and Stable Electrocatalytic Hydrogen Evolution. Small, 2018, 14(17), 1800340.

15. Jin, Y.; Yue, X.; Shu, C.; Huang, S.; Shen, P. K. Three-dimensional porous $MoNi_4$ networks constructed by nanosheets as bifunctional electrocatalysts for overall water splitting. Journal of Materials Chemistry A, 2017, 5(6), 2508-2513.

16. Karuppasamy, K.; Jothi, V. R.; Vikraman, D.; Prasanna, K.; Maiyalagan, T.; Sang, B.; Yi, S.; Kim, H. Metal-organic framework derived NiMo polyhedron as an efficient hydrogen evolution reaction electrocatalyst. Applied Surface Science, 2019, 478, 916-923.

17. Zhang, Y.; Wang, Y.; Jia, S.; Xu, H.; Zang, J.; Lu, J.; Xu, X. A hybrid of NiMo-Mo_2C/C as non-noble metal electrocatalyst for hydrogen evolution reaction in an acidic solution. Electrochimica Acta, 2016, 222, 747-754.

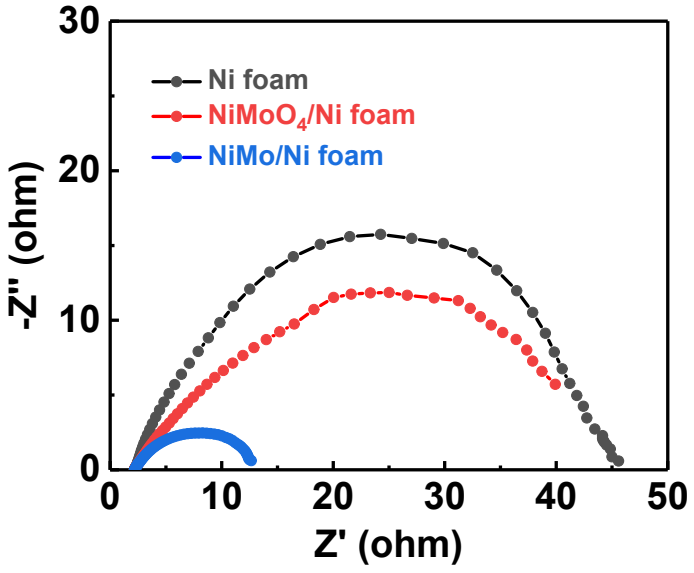

Fig. S12 Nyquist plots of Ni foam, NiMoO4/Ni foam, and NiMo/Ni foam.

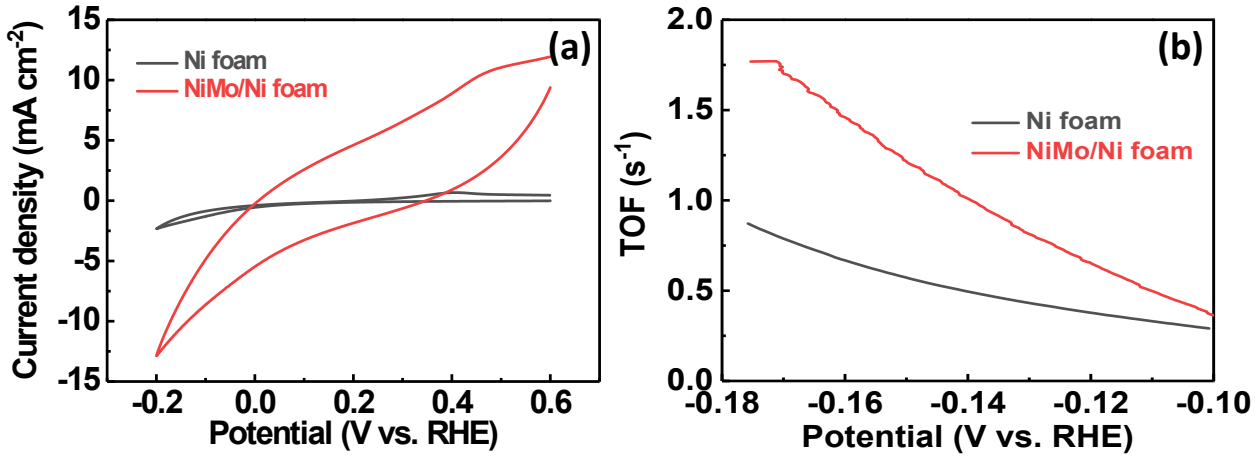

Fig. S13 (a) CV curves for Ni foam and NiMo/Ni foam in 0.5 M PBS (pH=7) at a scan rate of 50 mV s^{-1}; (b) comparison of the TOFs of Ni foam and NiMo/Ni foam.

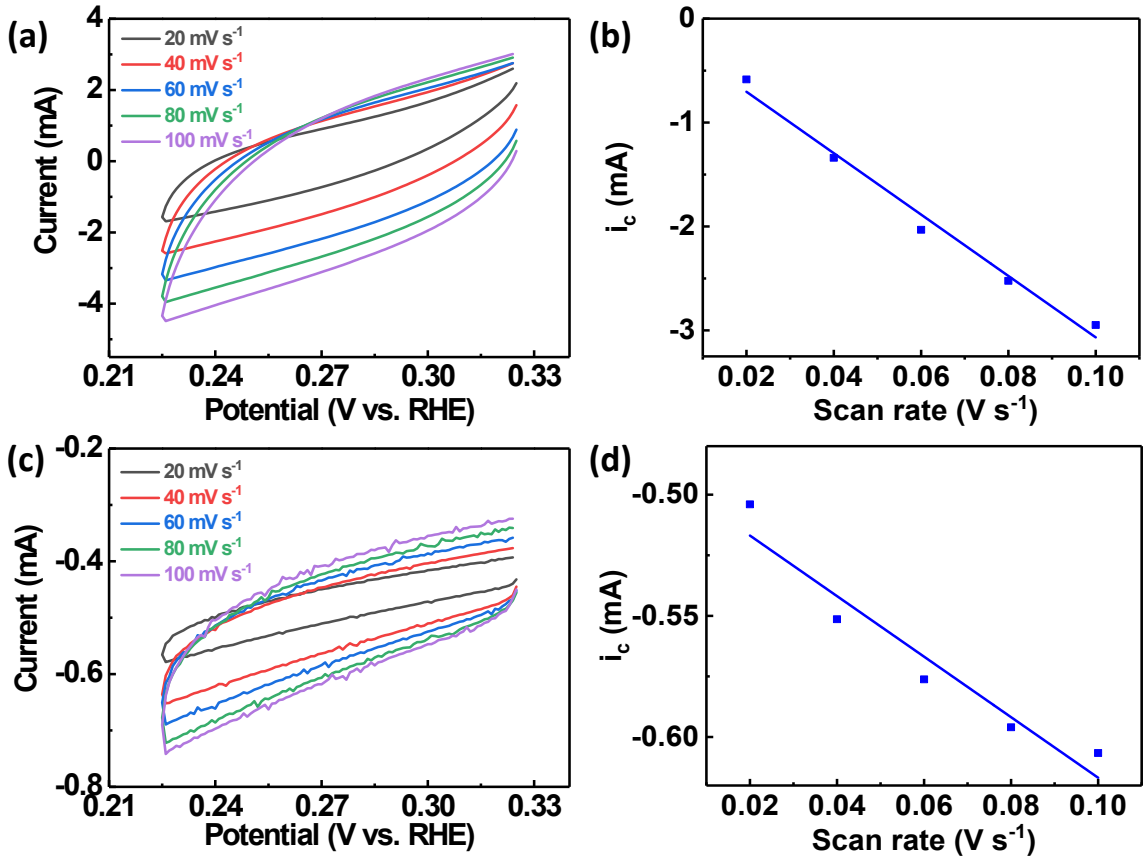

Fig. S14 CV curves of NiMo/Ni foam (a) and C-NiMo/Ni foam (c) at different scan rates; double-layer charging currents of NiMo/Ni foam (b) and C-NiMo/Ni foam (d) at 0.275 V (vs. RHE) with respect to the potential scan rate.

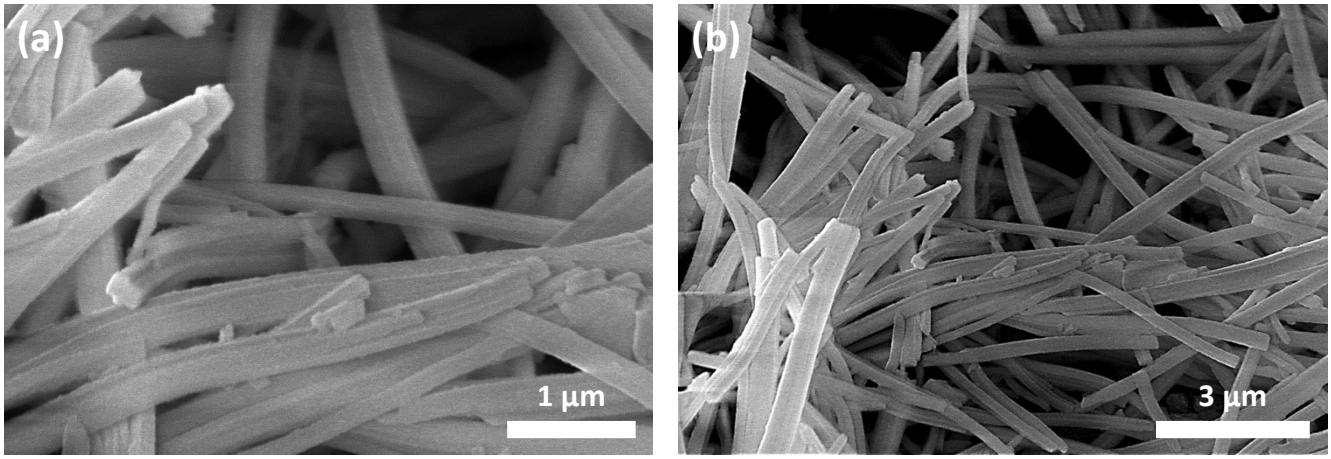

Fig. S15 (a, b) FESEM images of NiMo/Ni foam after a long-term HER stability test.